
**Liquid Crystals**
Publication details, including instructions for authors and subscription information:
http://www.informaworld.com/smpp/title~content=t713926090

# Dielectric evidence of an electroclinic effect in the cholesteric phase near a N * -SmA-SmC * multicritical point

J. Hmine[a]; C. Legrand[b]; N. Isaert[c]; H. T. Nguyen[d]
[a] Laboratoire de Physique de la Matière Condensée, Université Hassan II, F.S.T., Mohammadia B.P. 146, Mohammadia, Maroc, [b] Laboratoire d'Etude des Matériaux et des Composants pour l'Electronique, E.A. 2601, Université du Littoral-Côte d'Opale B.P. 717, Calais, France, [c] Laboratoire de Dynamique et Structures des Matériaux Moléculaires, U.R.A. n° 801, Université de Lille 1, 59655 Villeneuve d'Ascq, France, [d] Centre de Recherche Paul Pascal, Université de Bordeaux 1, 33600 Pessac, France,

Online publication date: 11 November 2010

**To cite this Article** Hmine, J. , Legrand, C. , Isaert, N. and Nguyen, H. T.(2003) 'Dielectric evidence of an electroclinic effect in the cholesteric phase near a N * -SmA-SmC * multicritical point', Liquid Crystals, 30: 2, 227 — 234
**To link to this Article: DOI:** 10.1080/0267829021000061123
**URL:** http://dx.doi.org/10.1080/0267829021000061123

LIQUID CRYSTALS, 2003, VOL. 30, NO. 2, 227–234



# Dielectric evidence of an electroclinic effect in the cholesteric phase near a N*–SmA–SmC* multicritical point

J. HMINE*
Laboratoire de Physique de la Matière Condensée, Université Hassan II, F.S.T., Mohammadia B.P. 146, Mohammadia, Maroc

C. LEGRAND
Laboratoire d'Etude des Matériaux et des Composants pour l'Electronique, E.A. 2601, Université du Littoral-Côte d'Opale B.P. 717, Calais, France

N. ISAERT
Laboratoire de Dynamique et Structures des Matériaux Moléculaires, U.R.A. n° 801, Université de Lille 1, 59655 Villeneuve d'Ascq, France

and H. T. NGUYEN
Centre de Recherche Paul Pascal, Université de Bordeaux 1, 33600 Pessac, France

(*Received 10 January 2002; in final form 16 September 2002; accepted 12 October 2002*)

Chiral liquid crystal materials ($n = 10$ and 11 homologues of a biphenyl alkyloxybenzoate series) exhibiting the ferroelectric smectic C phase (SmC*), the smectic A phase (SmA) and the cholesteric phase (N*) have been studied by structural, electro-optical and dielectric methods. In the structural study, helical pitch, tilt angle and polarization measurements show that the N*–SmC* and the N*–SmA phase transitions appear near a N*–SmA–SmC* multicritical point. In the dielectric measurements, we have studied the soft mode in the SmC* and SmA phases. We have detected a new relaxation mechanism in the N* phase of these compounds. The temperature dependence of this relaxation process is similar to that of the classical soft mode observed in the SmA phase. This dielectric relaxation process is attributed to an electroclinic effect in the N* phase near a N*–SmA–SmC* multicritical point. From the experimental data (structural and dielectric studies), we have evaluated the soft mode rotational viscosity, the $\alpha$-coefficient of the free energy and the electroclinic coefficient for the SmA and N* phases.



## 1. Introduction

The electroclinic effect near a SmC*–SmA phase transition is now well known [1]. For example, much data has been reported on this effect in the SmA and SmC* phases from optical observations made using planars thin cells [2, 3]. This effect corresponds to an electrically induced tilt of the molecules: the electric field is applied in the smectic plane and the molecules tilt in a plane perpendicular to the field direction. At a fixed temperature, the induced tilt is proportional to the amplitude of the applied electric field. At higher levels, saturation of the induced tilt may occur. At a given amplitude of the electric field, the induced tilt and the switching time are higher at a SmC*–SmA phase transition and decrease far below this phase transition. Such a temperature behaviour is well explained by the Landau model of the SmC*–SmA phase transition. The soft mode of the transition corresponds, in this model, to in-phase fluctuations of the tilt angle (electroclinic effect) and of the polarization. These fluctuations result in a Debye-type relaxation process. Therefore, the electroclinic effect can be indirectly detected by dielectric methods.

An electroclinic effect in the N* phase has been observed optically and measured by Komitov *et al.* [4] and by Lee and Patel [5] for mixtures exhibiting a large N* pitch near the N*–SmA and N*–SmC* phase transitions. In a previous paper, we described a dielectric relaxation process in the N* phase for pure chiral

*Author for correspondence; e-mail: hmine@uh2m.ac.ma

*Liquid Crystals* ISSN 0267-8292 print/ISSN 1366-5855 online © 2003 Taylor & Francis Ltd
http://www.tandf.co.uk/journals
DOI: 10.1080/0267829021000061123

homologues, $n = 8$ and $n = 10$, of the series of biphenylyl alkyloxybenzoates given in table 1 [6]. The temperature-dependences of the characteristic parameters (dielectric strength and relaxation frequency) of this relaxation process are similar to those of the soft mode classically observed in the SmA phase. We have interpreted this relaxation mechanism observed in the N* phase as an electroclinic effect near a N*–SmA transition for $n = 10$ or near a N*–SmC* transition for $n = 8$. The relatively high amplitude of this effect is connected with the proximity of a N*–SmA–SmC* multicritical point established by isochoric thermobarometric measurements [7]. Marcerou has theoretically predicted this effect in generalizing Meyer's theory of ferroelectric liquid crystals [8]. He has shown that the trilinear coupling between the smectic layers, the tilt angle and the electric polarization, is responsible for the electroclinic effect in the SmC*, SmA and N* phases, especially in the vicinity of a N*–SmA–SmC* multicritical point.

In this paper, we complete the experimental data by a characterization of the homologue with $n = 11$ by helical pitch, tilt angle, polarization and dielectric measurements. The results are compared with these obtained for the $n = 10$ compound. We also show that the electroclinic effect in the N* phase of these two compounds is important and has a similar order of magnitude.

## 2. Biphenyl alkyloxybenzoate series

The synthesis details for these new homologues series have already been published [6]. The phase sequences and transition temperatures determined both by thermal microscopy (Mettler FP5) and by differential scanning calorimetry (Perkin-Elmer DSC7) are presented in table 1. From this table, it can be seen that the first three compounds of the series ($n = 7$ to 9) exhibit no SmA phase and show the sequence phase Cr–SmC*–N*–BP–I. When the alkyloxy chain length increases ($n = 10$ to 12), the SmA phase appears between the SmC* and N* phases. The temperature range of the SmA phase increases with the length of the alkyloxy chain. This temperature range is 1 and 3°C, respectively, for $n = 10$ and $n = 11$.

From the pressure–temperature phase diagrams deduced from thermobarograms ($P$–$T$ recording), it has been shown that the transitions N*–SmC* and N*–SmA–SmC* appear near a N*–SmA–SmC* multicritical point for two of the homologues: $n = 8$ and $n = 10$ [6, 7].

## 3. Structural studies

### 3.1. *Helical pitch measurements*

The helical pitch values for the two compounds were measured by the Grandjean–Cano method [9, 10] with prismatic planar aligned samples in the N* phase and prismatic pseudo-homeotropic samples in the SmC* phase. We could obtain excellent sample orientations forming regular steps in the N* and SmC* phases allowing helical pitch measurements.

The temperature dependence of the pitch is rather classical. Figure 1 (*a*) gives the pitch variation versus temperature for $n = 10$. In the N* phase far above the N*–SmA transition, the pitch is very short: $p \sim 0.18\,\mu m$, and gives coloured selective reflection of light. On cooling, the N* pitch grows regularly up to 2.3 μm near the SmA phase and diverges at the N*–SmA transition.

In the SmC* phase, the pitch is relatively low far below $T_C$: $p \sim 1.4\,\mu m$, and increases up to 2.3 μm when the temperature increases. Close to the SmC*–SmA phase transition, the Grandjean–Cano defects may become invisible because the rotatory power cancels with the tilt angle. The 'flat drop' method [11] was then used and

Table 1. Chemical formulae, phase sequences and transition temperatures (°C) for the homologues of the biphenyl benzoate series. Cr = crystalline phase; Sm = smectic phases A, C*; N* = cholesteric phase; BP = blue phase; I = isotropic phase. () = monotropic transition.

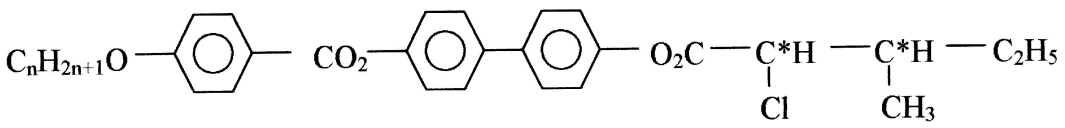


| *n* | Cr | | Sm | | SmC* | | SmA | | N* | | BP | | I |
|---|---|---|---|---|---|---|---|---|---|---|---|---|---|
| 7 | • | 100 | • | (52) | • | 134 | — | | • | 166 | • | 166.1 | • |
| 8 | • | 88 | — | | • | 138 | — | | • | 165.5 | • | 166.5 | • |
| 9 | • | 89 | — | | • | 142 | — | | • | 162 | • | 162.1 | • |
| 10 | • | 88 | — | | • | 143 | • | 144 | • | 159 | • | 160 | • |
| 11 | • | 88 | — | | • | 146 | • | 149 | • | 157 | • | 157.1 | • |
| 12 | • | 81 | — | | • | 145.5 | • | 150 | • | 154 | • | 154.5 | • |

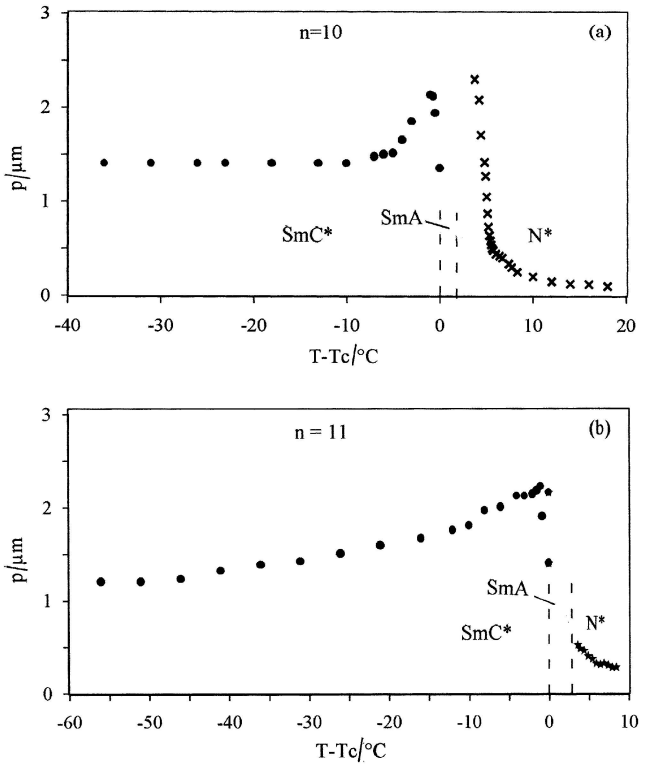


Figure 1. Pitch temperature dependence in the SmC* and N* phases for $n = 10$ (*a*) and $n = 11$ (*b*).

gives the limiting value of the pitch at the transition temperature for this material; we estimate this value at 1.3 µm near the SmC*–SmA transition, showing the interest of this method in this delicate case.

Figure 1 (*b*) shows the evolution of the pitch as a function of temperature for $n = 11$. This compound exhibits the same kind of behaviour in the N* and SmC* phases. In conclusion, the pitch behaviours are characteristic of the existence of the SmA phase between the SmC* and N* phases for these two materials.

### 3.2. *Electro-optical properties*

To study the tilt angle $\theta$ and the spontaneous polarization $\mathbf{P}_S$, we used the surface stabilised ferroelectric liquid crystal configuration (SSFLC) [12]. The sample thickness was about 3 µm estimated by the Newton fringe method. In order to measure the temperature variation of the tilt angle, a low frequency and high amplitude electric field ($E = 5\ \text{V}\ \mu\text{m}^{-1}$; $F = 0.2$ Hz) was applied to the samples. The spontaneous polarization measurements used the same experimental set-up as for the tilt angle measurements, the amplitude of the electric field necessary to saturate the polarization being around $6\ \text{V}\ \mu\text{m}^{-1}$ and the frequency about 1 kHz. Reversal of the electric field reverses the polarization. The electrical charge carried gives the macroscopic polarization.

#### 3.2.1. *Tilt angle*

In figure 2, we see that at low temperatures and far from the SmC*–SmA phase transition, the tilt angle saturates to a value of 35°. When the temperature is increased the tilt angle decreases as far as the SmC*–SmA transition temperature, where it is approximately 15° and 10°, respectively, for $n = 10$ and $n = 11$. It was interesting to study the effect of electric field strength on the tilt angle (figure 3) for the material $n = 11$. These results show that the tilt angle saturates at a value close to 35° for two values of the electric field ($V = 5$ and 10 V), while it was found to decrease at the SmC*–SmA transition to 5° and 10° for $V = 5$ and 10 V, respectively. This behaviour is classical and can be explained by the coupling of the tilt angle with an applied electric field. This coupling is strong enough to induce tilt angles of a few degrees at the SmC*–SmA transition [13].

#### 3.2.2. *Spontaneous polarization*

The results obtained for the two materials are given in figure 4, indicating that both compounds have a high spontaneous polarization at low temperatures; we obtained, at $T_C - T = 50$°C, 160 and 150 $\text{nC}\,\text{cm}^{-2}$,

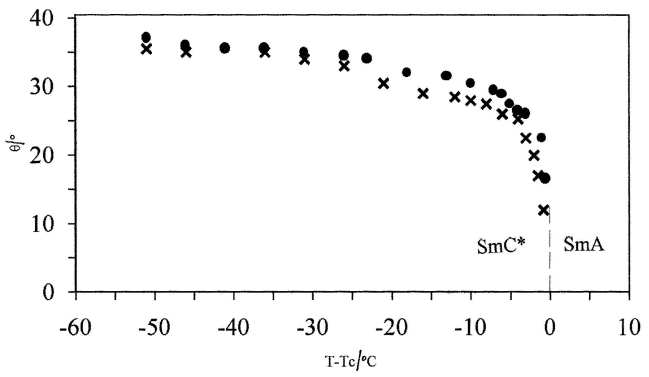


Figure 2. Tilt angle temperature dependence for $n = 10$ (●) and $n = 11$ (×).

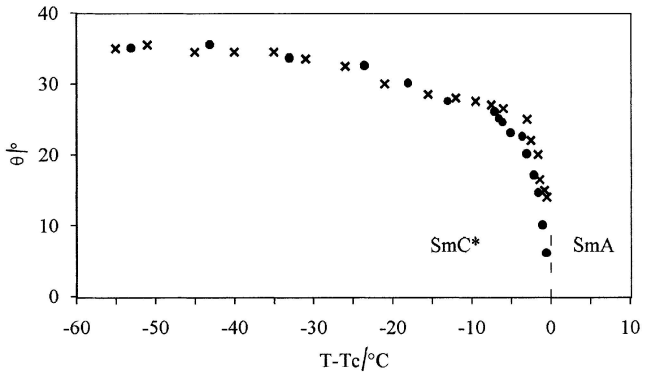


Figure 3. Tilt angle as a function of applied voltage and temperature for $n = 11$: $V = 5$ V (●) and $V = 10$ V (×).

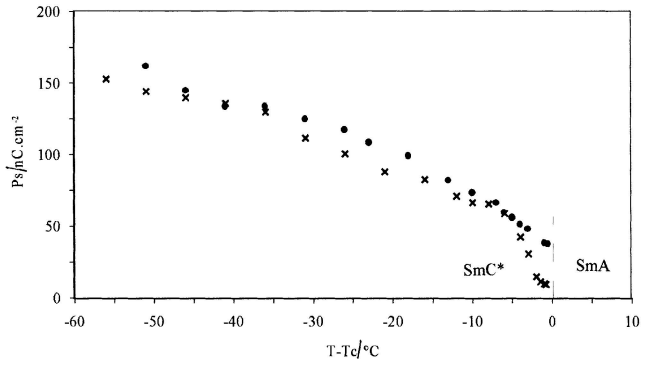


Figure 4. Temperature dependence of the spontaneous polarization for $n = 10$ (●) and $n = 11$ (×).

respectively, for $n = 10$ and $n = 11$. To a first approximation, this parameter is proportional to the tilt angle and decreases at the approach of the SmA phase.

It is interesting to note that near the SmC*–SmA transition the spontaneous polarization is much greater for $n = 10$ ($40\,\mathrm{nC\,cm^{-2}}$) than for $n = 11$ ($10\,\mathrm{nC\,cm^{-2}}$). This difference could be explained by the influence of the alkyloxy chain length in the proximity of the multicritical point and by the existence of a much more prominent apparent optical tilt angle for the $n = 10$ compound.

## Dielectric studies

The dielectric measurements were made with a planar orientation of the sample, in the frequency range 5 Hz–1 MHz, using a previously described experimental procedure [6, 14]. The sample texture in the N* phase is the Grandjean texture (not finger-print): the molecular axis (helical axis) is parallel (perpendicular) to the electrode surfaces. This orientation corresponds to a planar orientation in the SmA and SmC* phases with the smectic layers perpendicular to the electrodes surfaces [15, 16]. The sample orientation was checked using polarizing microscopy with reflected light.

The cell thickness, 30 µm, was chosen to be much higher than the pitch value to obtain a planar wound geometry in the SmC* phase. The measurements were made in two steps: without superimposition of a d.c. bias to the measurement electric field, and with superimposition of a d.c. bias to unwind the helix in the SmC* phase.

### 4.1. *Dielectric study without a d.c. bias*

Without a d.c. bias, we observed one relaxation domain in the SmA phase for these two materials. We also detected another relaxation process at higher frequencies in the N* phase. Its dielectric strength was much lower than that of the relaxation process attributed to the Goldstone mode [17, 18] and it strongly increased near the SmA–SmC* phase transition, whereas the relaxation frequency showed reverse behaviour (figures 5 and 6).

In the SmA phase, the inverse of the dielectric strength and relaxation frequency depend linearly on temperature. This process corresponds to 'in-phase' fluctuations of the amplitude of the order parameters (the electroclinic effect for the tilt angle) and is the so-called 'soft mode' [19, 20]. The temperature dependence of the relaxation frequency $f_S$ of the soft mode in the SmA phase shows that this frequency varies in the range 6–45 kHz for $n = 10$—figure 5(*b*)—and 20–100 kHz for $n = 11$, see figure 6(*b*). These values are higher than those of the relaxation frequency of the Goldstone mode $f_G$ [21, 22] measured near the SmC*–SmA phase transition.

The same behaviour is observed in the N* phase near the N*–SmA phase transition, with a continuity of the characteristic parameters observed for the two materials. Indeed, in the N* phase, there are linear evolutions of both the inverse of the amplitude $\Delta\varepsilon_s^{-1}(T)$ and the relaxation frequency $f_s(T)$. The continuation of the characteristic parameters from the SmA phase to the N* phase is marked by abrupt changes of slope. We thus obtained, on the one hand, $\mathrm{d}\varepsilon_s^{-1}/\mathrm{d}T = 0.25^{\circ}\mathrm{C}^{-1}$ (SmA), $0.55^{\circ}\mathrm{C}^{-1}$ (N*); and $\mathrm{d}f_s/\mathrm{d}T = 70\,\mathrm{kHz\,^{\circ}C^{-1}}$ (SmA); $150\,\mathrm{kHz\,^{\circ}C^{-1}}$ (N*)

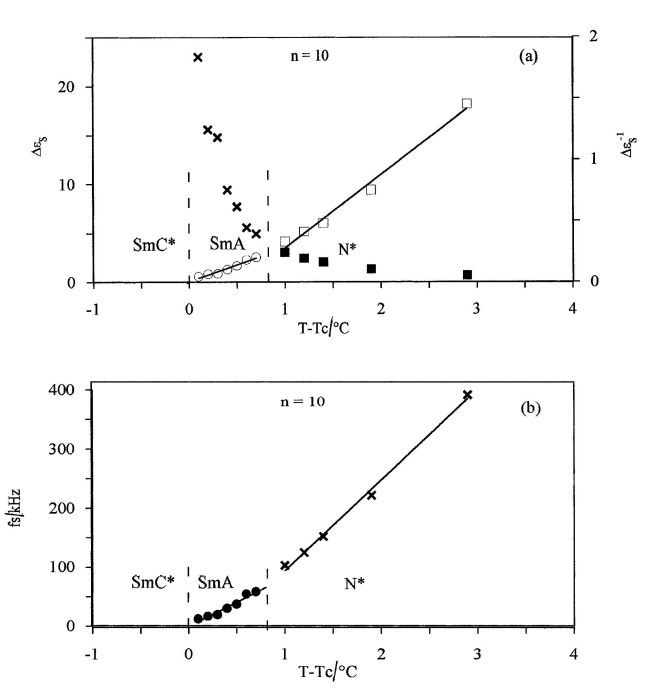


Figure 5. Temperature dependence of the dielectric strength (*a*) and relaxation frequency (*b*) of the soft mode in the SmA phase and of the relaxation mechanism observed in the N* phase for $n = 10$. The inverse dielectric strength (*a*) is also reported. Measurements were made without d.c. bias.

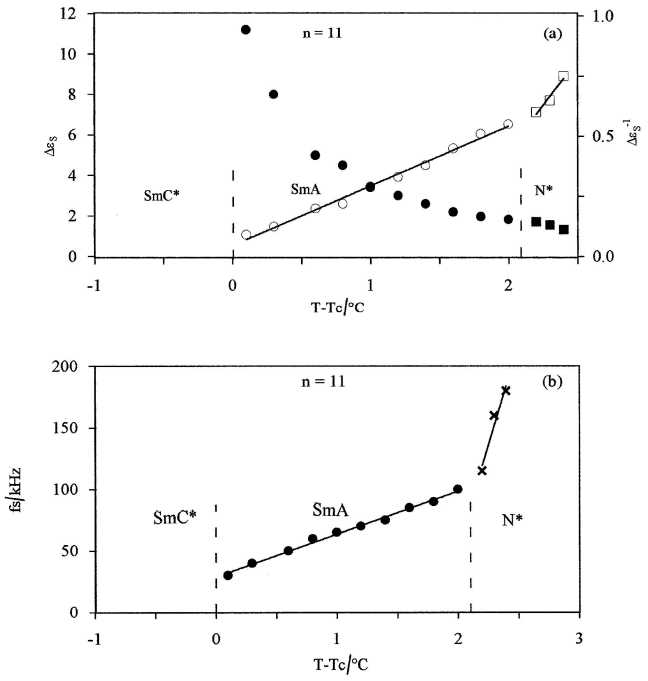


Figure 6. Temperature dependence of the dielectric strength (*a*) and relaxation frequency (*b*) of the soft mode in the SmA phase and of the relaxation mechanism observed in the N* phase for $n = 11$. The inverse dielectric strength (*a*) is also reported. Measurements were made without d.c. bias.

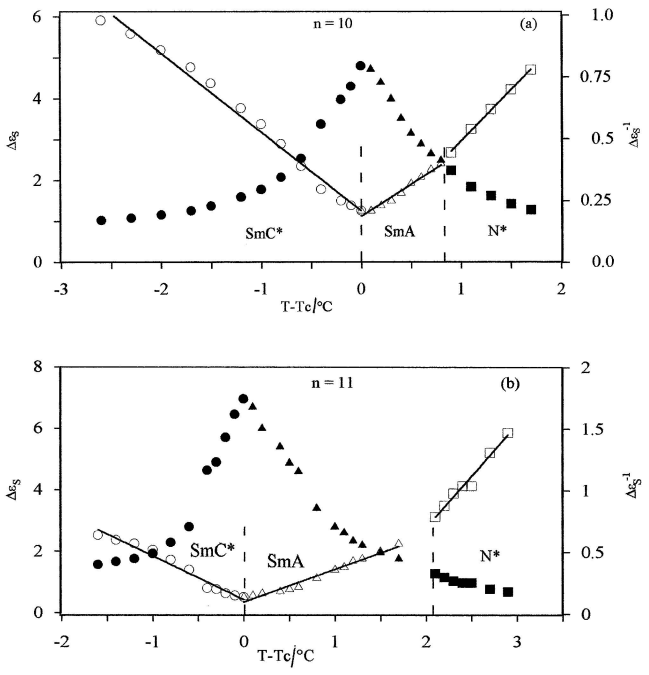


Figure 7. Temperature dependence of the dielectric strength and inverse dielectric strength of the soft mode in the SmC* and SmA phases and of the relaxation process observed in the N* phase for $n = 10$ (*a*) and $n = 11$ (*b*). Measurements were made with a d.c. bias of 1 V $\mu m^{-1}$.

for $n = 10$. On the other hand the slopes for the $n = 11$ material were $0.25^{\circ}C^{-1}$ (SmA), $0.75^{\circ}C^{-1}$ (N*); and $35\,kHz\,^{\circ}C^{-1}$ (SmA), $320\,kHz\,^{\circ}C^{-1}$ (N*).

These experimental data confirm our previous results, and this relaxation process can be attributed to an electroclinic effect in the N* phase. It is important to note that this effect is detected in pure chiral compounds by the dielectric method.

### 4.2. *Dielectric study with a d.c. bias*

In order to obtain a complete characterization of the soft mode in the SmC* phase, we superimposed a d.c. bias on the measurement electric field. A d.c. bias of 30 V was necessary to unwind the helix in the SmC* phase. Then, the Goldstone mode disappears and only one relaxation process corresponding to the soft mode is observed. This process is still detected in the SmA and N* phases. Temperature dependences of the dielectric strength and the relaxation frequency obtained for both materials are given in figures 7 and 8.

The dielectric strength has a maximum at the SmC*–SmA phase transition, whereas the relaxation frequency has a reversed behaviour. Furthermore, in the proximity of the SmC*–SmA transition, the reverse dielectric strength and the frequency of the soft mode in the SmC* and SmA phases are linear functions of temperature. These qualitative behaviours are in very good agreement with the theoretical model predictions [23], and have already been observed and studied by other authors for many materials [21, 22, 24].

We can also see from figures 5 (*a*), 6 (*a*) and 7 that the dielectric strength $\Delta\varepsilon_S$ at the SmC*–SmA phase transition without a d.c. bias is larger than $\Delta\varepsilon_S$ measured with a d.c. bias: $\Delta\varepsilon_S(E = 0) = 26$, $\Delta\varepsilon_S(E = 1\ V\ \mu m^{-1}) = 5$ for $n = 10$; and $\Delta\varepsilon_S(E = 0) = 11$, $\Delta\varepsilon_S(E = 1\ V\ \mu m^{-1}) = 7$ for $n = 11$. On the other hand, the relaxation frequency of the soft mode $f_S$ at $T = T_C$ measured without a d.c. bias is lower than $f_S$ measured with a d.c. bias: $f_S(E = 0) = 6\,kHz$, $f_S(E = 1\ V\ \mu m^{-1}) = 35\,kHz$ for $n = 10$; and $f_S(E = 0) = 30\,kHz$, $f_S(E = 1\ V\ \mu m^{-1}) = 40\,kHz$ for $n = 11$. Such differences (already observed [22, 23]) are mainly due to the electroclinic effect and are enhanced by a high value of the d.c. bias.

The process observed at high frequencies in the SmA phase is still detected in the N* phase near the N*–SmA transition. As can be seen from figures 7 and 8, the reverse strength and the relaxation frequency for this process are also linear functions of temperature. It is interesting to compare the experimentally deduced values of the slopes $df_S/dT$ in the SmA and N* phases (table 2). A great difference in the slope values confirms that the relaxation process is observed in the N* phase.

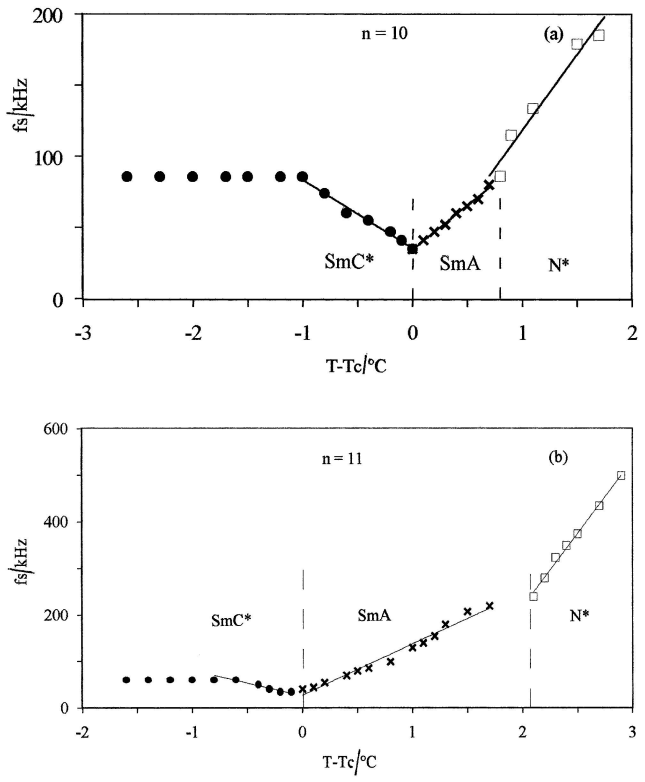


Figure 8. Temperature dependence of the relaxation frequency of the soft mode in the SmC* and SmA phases and of the relaxation process observed in the N* phase for $n = 10$ (*a*) and $n = 11$ (*b*). Measurements were made with a d.c. bias of 1 V $\mu m^{-1}$.

Table 2. Experimental slope values for the relaxation frequency (kHz $^{\circ}C^{-1}$) in the SmA and N* phases for $n = 10$ and 11 ($E = 1$ V $\mu m^{-1}$).

| Compound ($n$) | $(df_S/dT)_{SA}$ /kHz $^{\circ}C^{-1}$ | $(df_S/dT)_{N^*}$ /kHz $^{\circ}C^{-1}$ |
|---|---|---|
| 10 | 60 | 120 |
| 11 | 95 | 370 |

## 5. Discussion

### 5.1. *Soft mode without a d.c. bias*

Using a simple Landau expansion, the dielectric strength $\Delta\varepsilon_S$ and the relaxation frequency $f_S$ of the soft mode in the SmA phase can be written as [23, 25]:

$$\Delta\varepsilon_S = \frac{4\pi\chi^2 C^2}{K_{33}q^2 + \alpha(T - T_C)} \tag{1}$$

$$f_S = \frac{K_{33}q^2 + \alpha(T - T_C)}{2\pi\gamma_{SA}} \tag{2}$$

where $q$ is the wave vector of the modulation in the SmC* phase, $K_{33}$ is the twist elastic constant, $\alpha$ is the usual coefficient in the temperature term of the Landau free-energy density expansion, $C$ is the temperature-independent coefficient of the piezoelectric bilinear coupling and $\gamma_{SA}$ is the rotational viscosity of the soft mode in the SmA phase.

As seen in these two equations, the inverse of the dielectric strength $1/\Delta\varepsilon_{SA}$ and the relaxation frequency $f_{SA}$ of the soft mode in the SmA phase decrease linearly with temperature when approaching $T_C$. This is in agreement with experimental behaviour. Using the slopes $d(\Delta\varepsilon_S^{-1})$, $df_S/dT$ and the experimental value of the coefficient $\chi C \sim P_s/\theta$ evaluated near $T_c$, we obtain an estimation for the soft mode rotational viscosity $\gamma_{SA}$ and the $\alpha$ coefficient. The rotational viscosities $\gamma_{SA}$ determined near the SmA–SmC* transition are of the same order of magnitude as those measured by other authors [22, 26] for many ferroelectric compounds. The values obtained for the rotational viscosities are: $\gamma_{SA} = 170$ and $\gamma_{SA} = 31$ mPa s, respectively, for $n = 10$ and $n = 11$.

We note that for $n = 10$, $\gamma_{SA}$ in the SmA phase is larger than the Goldstone rotational viscosity $\gamma_G$ in the SmC* phase [6]. The same remark has been made by the Swedish group [26], who reported the temperature dependence of the soft mode and the Goldstone mode rotational viscosities in the SmA and SmC* phases. We can also evaluate the $\alpha$ coefficient: $\alpha = 6.4 \times 10^4$ N m$^{-2}$ K$^{-1}$ for $n = 10$, and $7 \times 10^3$ N m$^{-2}$ K$^{-1}$ for $n = 11$.

### 5.2. *Electroclinic effect in the SmA and N* phases*

We shall now determine the relaxation time $\tau_S = 1/2\pi f_s$ and the electroclinic coefficient $e_C$ in the SmA phase around the N*–SmA–SmC* phase sequences. From the Landau free energy expansion, the temperature dependence of the electroclinic effect coefficient $e_C$ can be derived from:

$$e_C = \frac{\Delta\varepsilon_S}{4\pi\chi C} = \frac{\chi C}{\alpha(T - T_C) + K_{33}q^2}. \tag{3}$$

Figure 9 shows the temperature dependence of the relaxation time in the SmA and N* phases for $n = 10$ and $n = 11$. In the SmA phase, for $n = 10$, $\tau_S$ increases with decreasing temperature and is found to vary between 13 and 2 µs, respectively, at the SmA–SmC* and SmA–N* transition temperatures, figure 9 (*a*). For $n = 11$, $\tau_S$ is about 5 µs at the SmA–SmC* phase transition and decreases to 1.5 µs when approaching the N* phase, figure 9 (*b*). This qualitative behaviour is in very good agreement with the theoretical prediction.

The temperature dependence of $e_C$ has the same behaviour as $\Delta\varepsilon_S(T)$ which increases quickly near $T_C$. Figure 9 shows the results obtained for the SmA and the N* phases for $n = 10$ and $n = 11$. For the $n = 10$ compound, the coefficient value is $8^{\circ}$ µm V$^{-1}$ at the SmA–SmC* phase transition; for $n = 11$, we obtained $e_C = 12^{\circ}$ µm V$^{-1}$ at the SmA–SmC* transition. For these two materials, the amplitude of the electroclinic effect

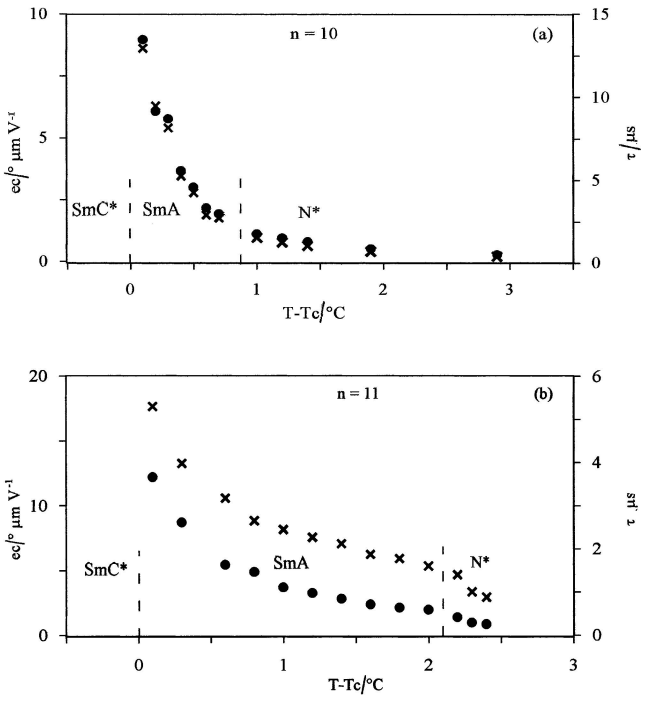


Figure 9. Temperature dependence of the relaxation time (×) and of the electroclinic effect (●) of the soft mode in the SmA phase and of the mechanism observed in the N* phase for $n = 10$ (*a*) and $n = 11$ (*b*).

has the same order of magnitude ($e_C = 2^\circ\ \mu m\ V^{-1}$) at the SmA–N* transition temperature.

The relaxation process observed in the N* phase is in perfect continuity with the soft mode observed in the SmA phase. This mechanism can thus also be attributted to an electroclinic effect in the N* phase. The continuity of the effect for both these materials across the transition between the SmA and N* phases means that this coefficient can reach $2^\circ\ \mu m\ V^{-1}$ in the N* phase close to the SmA–N* transition.

The relaxation mechanism detected in the N* phase persists only in a narrow temperature range at the vicinity of the SmA–N* transition. Thus the electroclinic effect vanishes at a temperature of 2°C and 0.3°C above the SmA–N* transition, respectively, for $n = 10$ and 11, whereas the temperature existence domain of the N* phase is about 13°C and 8°C, respectively, for $n = 10$ and 11. This explains why the electroclinic effect in the N* phase is detectable only in the proximity of a N*–SmA–SmC* multicritical point.

The values obtained in the N* phase are much larger than those obtained by Li *et al.* [27], Lee and Patel [5] ($10^{-2\,\circ}\ \mu m\ V^{-1}$) or Extebarria and Zubia [28] ($0.5 \times 10^{-2\,\circ}\ \mu m\ V^{-1}$ ) in the N* phase near the N*–SmA transition. More recently, Blinov *et al.* [29] measured, by pyroelectric response studies, a relatively lower electroclinic coefficient ($e_C = 0.8^\circ\ \mu m\ V^{-1}$) in the chiral nematic phase (N*) close to a first order N*–SmC* phase transition. The electroclinic effect in the N* phase near the N*–SmC* transition has also been measured by Komitov *et al.* [4] in mixtures exhibiting a large N* pitch (helical wave vector $q \sim 0$). We note that the low values of the pitch in our pure chiral materials do not allow us to make unwound samples in order to use the same optical method.

The amplitude of the electroclinic coefficient is connected with the piezoelectric coupling term $\chi C$ and so to the spontaneous polarization in the SmC* phase. Therefore, for our materials, which have a very high polarization ($\mathbf{P}_S = 160$ and $150\ nC\,cm^{-2}$, respectively, for $n = 10$ and $n = 11$), the amplitude of this electroclinic effect can grow to high values especially near the SmC*–SmA and SmA–N* phase transitions. This can also be explained by the proximity of the N*–SmA–SmC* multicritical point and due to the existence of local smectic order in the N* phase (cybotactic groups [4]) enhanced by the proximity of the N*–SmA–SmC* multicritical point.

The relaxation process detected and studied in the N* phase for these two materials has the same behaviour as the soft mode classically observed in the SmA phase. It is continuous at the transition from the SmA–N* phase transition. For these reasons, we attribute this relaxation mechanism to an electroclinic effect in the N* phase.

## 6. Conclusion

Helical pitch, tilt angle, polarization and dielectric measurements on two homologues ferroelectric liquid crystals exhibiting the N*–SmA–SmC* phase sequence have been carried out as a function of temperature. One dielectric relaxation process was detected at relatively high frequency in the N* phase; this relaxation process was attributed to an electroclinic effect in this phase. The amplitude of this effect was found to be much greater than that measured optically by several authors in other compounds. This is well described qualitatively by the existence of local smectic order emphasized by the proximity of the N*–SmA–SmC* multicritical point. The soft mode rotational viscosity, the $\alpha$ coefficient of the free energy, the response time and the electroclinic coefficient were also calculated using a simple Landau model.

## References

[1] Garoff, S., and Meyer, R. B., 1977, *Phys. Rev. Lett.*, **38,** 848.
[2] Dupont, L., Glogarova, M., Marcerou, J. P., Nguyen, H. T., Destrade, C., and Lejcek, L., 1991, *J. Phys. II, Fr.*, **51,** 787.
[3] Ruozi, Q., John, T. H., and Hark, S. K., 1988, *Phys. Rev. A*, **38,**1653.

[4] Komitov, L., Lagerwall, S. T., Stebler, B., Andersson, G., and Flatischler, K., 1991, *Ferroelectrics*, **114,** 167.
[5] Lee, S. D., and Patel, J. S., 1991, *Phys. Rev. Lett. A*, **155,** 435.
[6] Legrand, C., Isaert, N., Hmine, J., Buisine, J. M., Parneix, J. P., Nguyen, H. T., and Destrade, C., 1992, *J. Phys. II Fr.*, **2,** 1545; Hmine, J., Legrand, C., Isaert, N., and Nguyen, H. T., 2001, in Proceedings of the 2nd Symposium on Surfaces-Interfaces in Electronic and Optoelectronic Components, 2001, Mohammadia, Maroc.
[7] Legrand, C., Isaert, N., Hmine, J., Buisine, J. M., Parneix, J. P., Nguyen, H. T., and Destrade, C., 1991, *Ferroelectrics*, **121,** 21.
[8] Marcerou, J. P., 1994, *J. Phys. II, Fr.*, **4,** 751.
[9] Grandjean, F., 1922, *C.R. Acad. Sci. Paris*, **172,** 71.
[10] Cano, R., 1968, *Bull. Soc. Fr. Min. Cryst.*, **91,** 20.
[11] Brunet, M., and Isaert, N., 1988, *Ferroelectrics*, **84,** 25.
[12] Clark, N. A., and Lagerwall, S. T., 1980, *Appl. Phys. Lett.*, **36,** 899.
[13] Bahr, C. H., and Heppke, G., 1987, *Liq. Cryst.*, **2,** 285.
[14] Legrand, C., and Parneix, J. P., 1990, *J. Phys. Fr.*, **51,** 787.
[15] Pavel, J., 1984, *J. Phys.*, **45,** 137.
[16] Dahl, I., and Lagerwall, S. T., 1984, *Ferroelectrics*, **58,** 2.
[17] Glogarova, M., Lejcek, L., Pavel, J., Janovec, V., and Fousek, J., 1982, *Czch., J. Phys.*, **32,** 943.
[18] Bawa, S. S., Biradar, A. M., and Chanadra, S., 1987, *Jpn. J. appl. Phys.*, **26,** 189.
[19] Blinc, R., and Zeks, B., 1978, *Phys. Rev. A*, **18,** 2.
[20] Martinot-Lagarde, Ph., and Durand, G., 1981, *J. Phys. Fr.*, **42,** 269.
[21] Filipic, C., Carlsson, T., Levestik, A., Zeks, B., Blink, R., Gouda, F., Lagerwall, S. T., and Skarp, K., 1988, *Phys. Rev. A*, **38,** 5833.
[22] Khened, S. M., Krishna Prasad, S., Shivkuma, B., and Sadashiva, B. K., 1991, *J. Phys. Fr.*, **2,**171.
[23] Carlsson, T., Zeks, B., Levstik, A., Filipic, C., Levstik, I., and Blinc, R., 1990, *Phys. Rev. A*, **42,** 877.
[24] Gouda, F., Andersson, G., Carlsson, T., Lagerwall, S. T., Skarp, K., Stebler, B., Filipic, C., Zeks, B., and Levstik, A., 1989, *Mol. Cryst. liq. Cryst. Lett.*, **6,** 151.
[25] Carlsson, T., Zeks, B., Levstik, A., Filipic, C., Levstik, I., and Blinc, R., 1987, *Phys. Rev. A*, **36,** 1484.
[26] Gouda, F., Skarp, K., and Lagerwall, S. T., 1991, *Mol. Cryst. liq. Cryst.*, **209,** 99.
[27] Li, Z., Di Lisi, G. A., Petschek, R. G., and Rosenblatt, C., 1990, *Phys. Rev. A*, **41,** 1997.
[28] Extebarria, J., and Zubia, J., 1991, *Phys. Rev. A*, **44,** 6626.
[29] Blinov, L. M., Beresnev, L. A., and Haase, W., 1996, *Ferroelectrics*, **181,** 211.